AGU PUBLICATIONS

Geophysical Research Letters

RESEARCH LETTER
10.1002/2016GL071859

Key Points:
- Detailed documentation of subtle primary coseismic surface faulting induced by moderate magnitude earthquake masked by later seismic event
- Contribute to the worldwide database of the moderate earthquakes surface faulting events in extensional domains

Supporting Information:
- Supporting Information S1

Correspondence to:
S. Pucci,
stefano.pucci@ingv.it

Citation:
Pucci, S., et al. (2017), Coseismic ruptures of the 24 August 2016, M_w 6.0 Amatrice earthquake (central Italy), *Geophys. Res. Lett.*, *44*, doi:10.1002/2016GL071859.

Received 5 NOV 2016
Accepted 4 JAN 2017
Accepted article online 6 JAN 2017

Coseismic ruptures of the 24 August 2016, M_w 6.0 Amatrice earthquake (central Italy)

S. Pucci[1], P. M. De Martini[1], R. Civico[1], F. Villani[1], R. Nappi[1], T. Ricci[1], R. Azzaro[1], C. A. Brunori[1], M. Caciagli[1], F. R. Cinti[1], V. Sapia[1], R. De Ritis[1], F. Mazzarini[1], S. Tarquini[1], G. Gaudiosi[1], R. Nave[1], G. Alessio[1], A. Smedile[1], L. Alfonsi[1], L. Cucci[1], and D. Pantosti[1]

[1]Istituto Nazionale di Geofisica e Vulcanologia, Rome, Italy

Abstract On 24 August 2016, a M_w 6.0 normal-faulting earthquake struck central Italy, causing about 300 fatalities and heavy damage. A geological survey collected the coseismic effects observed at the surface in order to evaluate two competing hypotheses about their nature: surface faulting versus gravitational deformation. We find that the most significant geological effect is a 5.2 km long alignment of ground ruptures along the Mount Vettore Fault System. These ruptures are independent from lithology, topography, morphology, and change in slope and exhibit an average dip-slip displacement of ~13 cm. Geometry, kinematics, and dimensional properties of this zone of deformation strongly lead us to favor the primary surface faulting hypothesis that fits well the predicted estimates from experimental scaling law relationships. Our study provides relevant hints for surface faulting in extensional domains, contributing to implement the worldwide database of the moderate earthquakes.

1. Introduction

On 24 August 2016, at 1:36 UTC, a M_w 6.0 earthquake, followed by a M_w 5.4 aftershock, hit the central Apennines belt, central Italy, nucleating at a depth of 8.2 km (Figure 1).

Focal mechanisms of the two main events show NW-SE striking normal faulting (Figure 1), the seismic sequence is confined into the upper 12 km of the crust and extends in NW-SE direction.

Both the events caused heavy damage in the old settlements within the epicentral area, resulting in 299 fatalities, thousands of injured, and more than 4500 displaced people [*Azzaro et al.,* 2016].

Numerous coseismic ground cracks occurred in the seismic sequence area, which deserve accurate investigations to discriminate their possible root: primary surface faulting (i.e., rupture directly connected to the deeper slip of the seismogenic source), secondary/sympathetic surface faulting (i.e., fault rupture not connected to the seismogenic source), or gravitational phenomena (i.e., shallow or deep-seated detachments of a seismo-induced landslide) [*dePolo et al.,* 1991].

The central Apennines chain is characterized by a Quaternary, NE-SW extensional regime overprinting NE verging thrust sheets [*Vai and Martini,* 2001], mostly made of Meso-Cenozoic carbonate rocks and Miocene flysch deposits. A dense array of NW-SE and NNW-SSE striking, mainly SW dipping, up to 30 km long, active normal fault systems accommodates ~3 mm/yr of extension across the chain [*D'Agostino*, 2014]. Among the main active tectonic structures in the area are the Vettore-Bove Mountains, the Laga Mountains, and the Norcia fault systems [*Galli et al.,* 2008] (Figure 1).

This region was repeatedly struck by $5.3 > M_w < 6.9$ earthquakes in the last 400 years with the largest local earthquake occurred in 1639 (Io 9–10 MCS, M_w 6.2) [*Rovida et al.,* 2016]. Also, it is the locus of others damaging moderate-sized earthquakes that struck central Italy in modern time: the M_w 5.8, 1979 Norcia to the west, the M_w 6.0, 1997 Umbria-Marche earthquake sequence to the north, and the M_w 6.1, 2009 L'Aquila sequence to the south.

Notwithstanding the considerable length of the Italian catalog of seismicity, the direct observation of coseismic surface ruptures is a quite rare phenomenon and usually is not the target of detailed studies. Within the Apennines chain, surface faulting has been assessed after the M_s 6.9, 1980 Irpinia earthquake [*Pantosti and Valensise,* 1990] and the catastrophic M_s 6.9–7.0, 1915 Avezzano earthquake [*Galadini and Galli,* 1999]. Instead, the occurrence of primary surface faulting was controversial after the M_w 6.0, 1997 Colfiorito

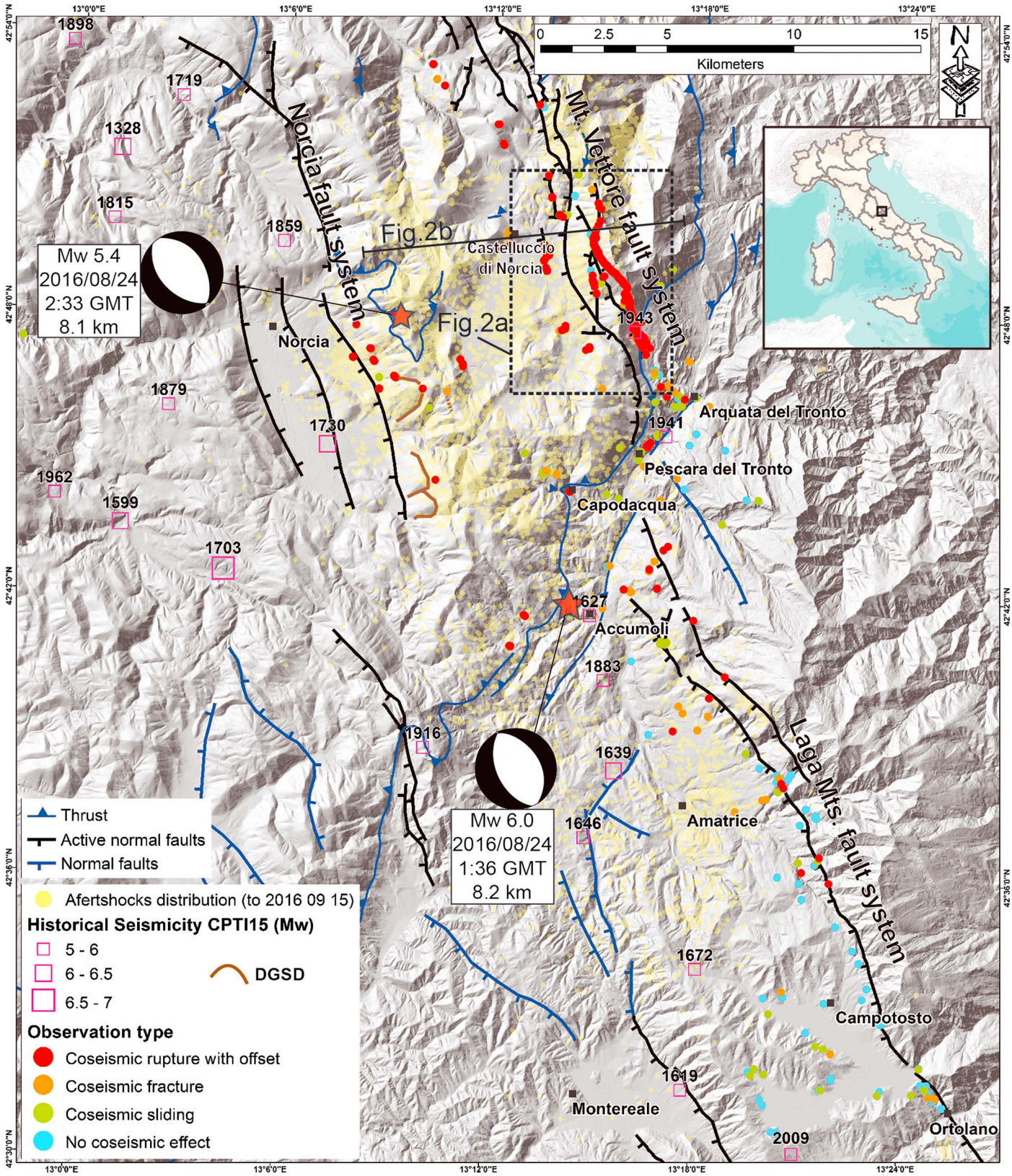

Figure 1. Location of the geological observations of coseismic effects [*EMERGEO Working Group*, 2016, modified]. Faults are compiled from *Centamore et al.* [1992] and *Pierantoni et al.* [2013]; active faults are from *Galli et al.* [2008]. The 2016 main shocks, aftershocks (until 15-9-2016) [*AMA_LOC Working Group*, 2016] and historical seismicity [*Rovida et al.*, 2016] are reported. Time Domain Moment Tensor focal mechanisms are from the INGV web page [http://cnt.rm.ingv.it].

earthquake [e.g., *Cello et al.,* 2000*; Cinti et al.,* 1999]. For the M_w 6.1, 2009 L'Aquila earthquake, seismological [*Valoroso et al.,* 2013], geodetic [*Atzori et al.,* 2009], and geologic data [*EMERGEO Working Group,* 2010] agree on the occurrence of surface faulting.

Low-to-moderate energy normal-faulting earthquakes capable of rupturing the surface are seldom observed worldwide [*Wells and Coppersmith,* 1994; *Stirling et al.,* 2013]. Therefore, a detailed analysis of the ground cracks is crucial to ascertain the presence of primary surface faulting and there is a major interest for earthquake geologists in characterizing the surface deformation. This is because it necessarily contributes to update the empirical relationships between magnitude and primary faulting expressions and is an important input for joint inversion models pointing to describe both seismic source and shallow-crust brittle deformation complexities.

Just before the submission of this manuscript, the area was struck again by a M_w 5.9 (26 October) and a M_w 6.5 (30 October) surface faulting events that are still under investigation and should be analyzed with regard to the following earlier observations.

2. Method

The data set of the coseismic geologic effects was collected in the epicentral area by the *EMERGEO Working Group* [2016], whose activity started soon after the main shocks. The use of devices equipped with software employing GPS, compass, and orientation sensors (Rocklogger©, www.rockgecko.com) allowed quick and accurate structural data collection and real-time sharing [*EMERGEO Working Group,* 2012]. The whole data were stored and managed in a georeferenced database by means of an ESRI ArcGIS platform. Additionally, low-altitude, easy deployable, aerial platforms (helikite and unmanned aerial vehicles,UAVs), together with a helicopter flight, enabled us to achieve an accurate documentation of the most prominent coseismic surface ruptures.

3. Data

More than 3200 observations of several types of surface coseismic effects were recorded within a ~750 km^2 wide area [*EMERGEO Working Group*, 2016]. In particular, 230 coseismic fractures (i.e., small open cracks exhibiting displacement $<$1 cm), 2600 coseismic ruptures (i.e., cracks exhibiting both vertical and horizontal displacements $>$1 cm), 160 medium- to small-sized coseismic landslides, 28 coseismic effects related to the shaking (e.g., clast extrusions, soil remobilization), three remobilized deep-seated gravitational slope deformations (DGSD) measurements and 130 observation points of known faults or landslides with no clear coseismic effect were collected (Figure 1).

The surveys carried out along the Laga Mountains Fault System (LFS), in the southern part, pointed out only some sparse data of discontinuous (maximum 300 m long) coseismic ruptures with small displacements (maximum 5 cm), mostly concentrated along its northern sector. Only a few ruptures exhibit a trend parallel to the mapped fault segments, whereas most of them do not have any systematic pattern. Conversely, in the central southern portion of the fault system, there is no clear surface coseismic fracturing or rupturing but several coseismic landslides, whose origin is possibly due to the low shear strength of the outcropping flysch. Some of them represent the reactivation of preexisting landslides, partly already known and mapped after the 2009 L'Aquila earthquake [*EMERGEO Working Group,* 2010].

On the other hand, in the northern part of the epicentral area, along the Mount Vettore Fault System (VFS), we mapped an almost continuous, N155° striking alignment of coseismic ruptures for an overall length of ~5.2 km, following the base of the cumulative tectonic scarps of Cima del Redentore and Vettoretto Mountains SW dipping normal faults (Figure 2a) whose total geologic throw is $>$500 m [*Pizzi et al.,* 2002] (Figure 2b). The fault scarp is made of bedrock at the footwall (mostly *Corniola Fm.,* Early Jurassic limestone), with highly fractured bedrock as well as various unconsolidated deposits at the hanging wall. The crosscut unconsolidated deposits display variable nature and thickness: they mainly consist of sharp-edged gravelly to pebbly matrix-supported (alluvial cones and colluvium with soil prone to gelifluction) and clast-supported deposits (graded, open-washed debris flows, and slope debris with no soil) derived from cryoclastic processes active on the steep bedrock slope.

A few additional coseismic ruptures parallel continuously to the southwestern fault splay of the VFS for more than 400 m, and another 1.2 km long discontinuous set is recognized at the slope foot (Figure 2a).

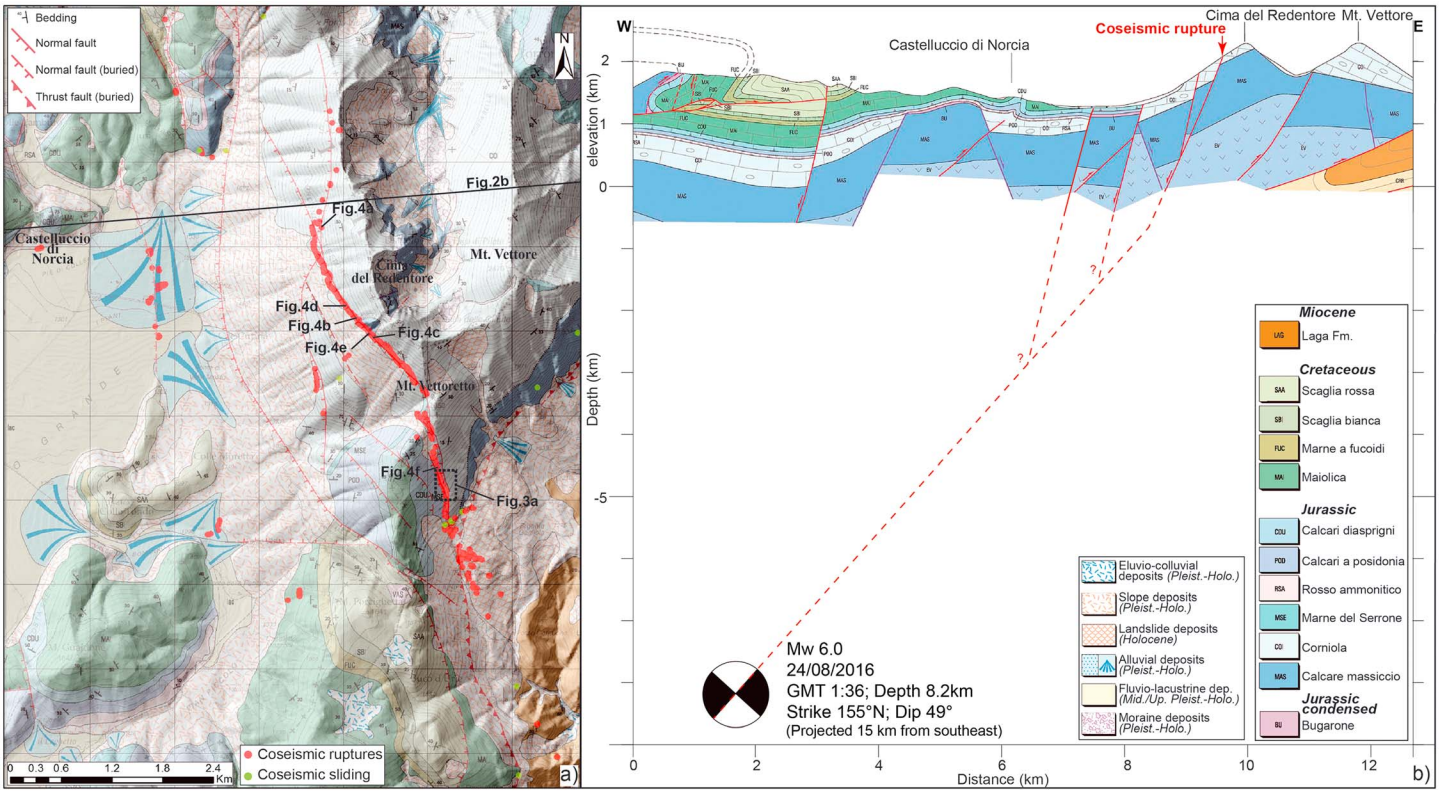

Figure 2. Coseismic ruptures with respect to the geological structures [*Pierantoni et al.,* 2013, modified] (Figures 1 and 2a for locations). (a) Distribution of the coseismic geological effects collected in the Mount Vettore area; (b) Geological cross section. The M_w 6.0 main shock projected along the SW dipping nodal plane is interpreted as the seismogenic fault plane. The upward extension of the plane and its connection with the VFS at shallow depth is sketched.

The overall ~5.2 km long coseismic deformation zone results from the envelope of single ruptures, up to 5.0–6.0 m long each, generally displaying a right stepping en échelon arrangement (Figure 3), with kinematically coherent oblique transfer zones, and a width not exceeding 5.0 m (typically $<$1.0 m). The orientation ranges of the different elements are as follows: (1) N125°–140° for the coseismic ruptures affecting unconsolidated deposits; (2) N105°–140° for coseismic fractures (with no appreciable displacement) affecting unconsolidated deposits; (3) N130°–175° for coseismic ruptures occurring on the bedrock fault planes (called "coseismic free faces," inset of Figure 3a). Along the steep southwestern flank of Mount Vettore, the coseismic rupture runs parallel to the elevation contours, while the ~2 km long alignment south of Mount Vettoretto is parallel to the local direction of the maximum slope and transects the mountainside (Figure 2a). Here it runs along the left flank of a small incision developed on the fractured fault hanging wall; notably, these ruptures locally cut the valley edges, causing a local reversal of the topography (Figure 3).

The coseismic rupture pattern is not controlled by the bedrock bedding strike, while locally it may follow preexisting joints near the fault planes (Figure 4a). The rupture trace preserves its trend, even when it cuts through debris cone apexes (Figure 4b), and keeps a close proximity to the bedrock fault planes. Where the bedrock fault plane is well preserved, the coseismic free face appears as a whitish, fresh ribbon at the base of the rejuvenated fault mirror (i.e., no soil shade and lack of lichens drape) (Figure 4c). Notably, we documented a coseismic rupture remobilizing an entire slice of fault breccia (Figure 4e). Each single element of the rupture maintains a general rectilinear path, regardless of the affected deposits (Figure 4d), linking aligned and dissected fault mirrors (Figure 4f).

The coseismic rupture shows the vertical component of movement always with the southwest side down, regardless of the affected topography. The extensional component of the movement is accommodated by vertical open cracks, closing at some decimeter of depth and mostly being shallow rooted onto a buried bedrock fault plane, 60°–80° dipping. The collected coseismic slip vectors show a predominant dip-slip

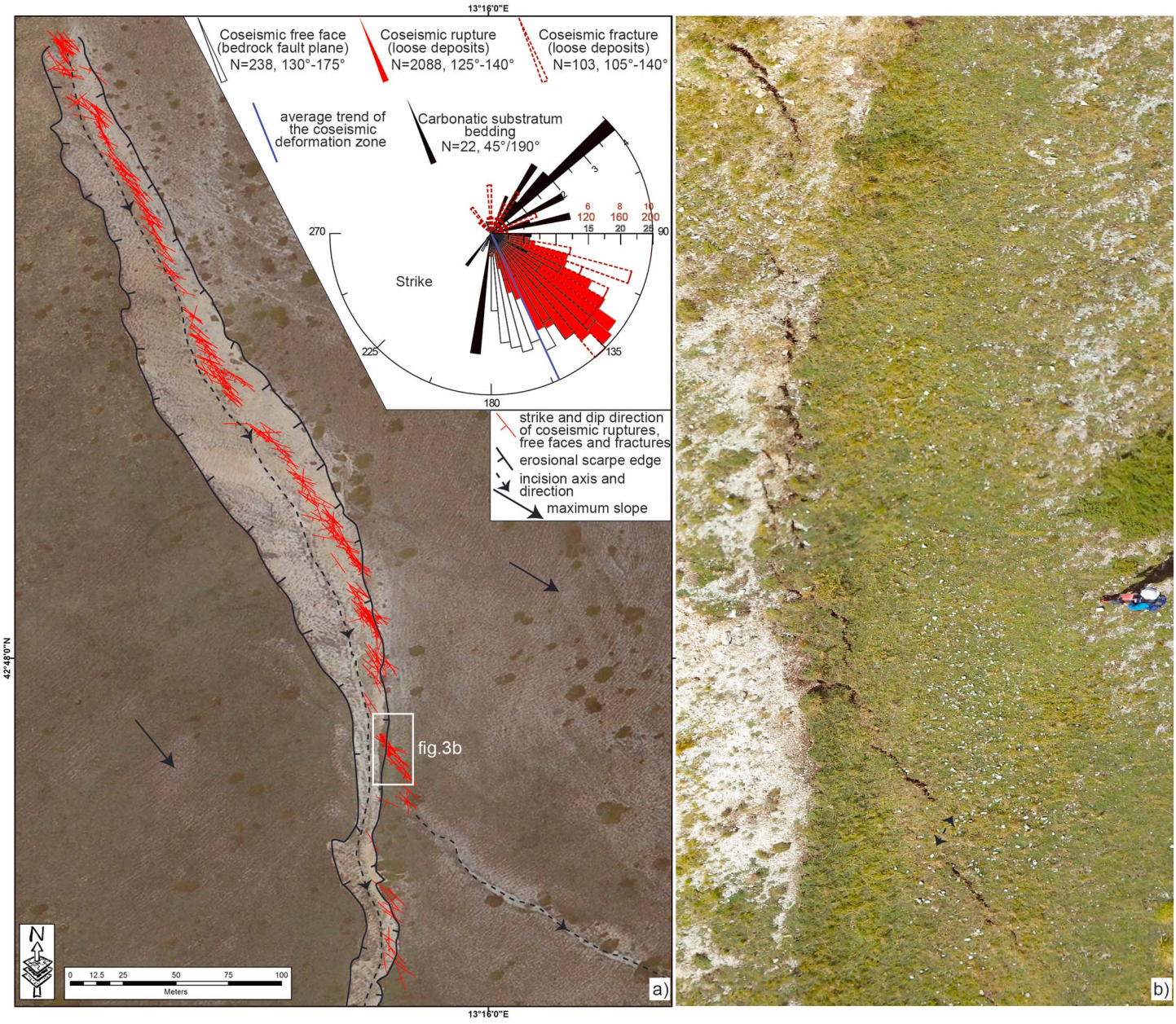

Figure 3. Pattern of the coseismic ruptures along the Mount Vettoretto flank (Figure 2a for location). (a) Particular of the rupture zone with the right stepping en échelon arrangement of the coseismic ruptures and related long-term geomorphic evidence. Rose diagram shows the strike of mapped features, bedrock bedding, and fault trace [*EMERGEO Working Group*, 2016]; (b) detail of the en échelon arrangement (helikite aerial view, man for scale).

component of the movement, parallel to the long-term slickensides observed on the bedrock fault planes (Figures 5a and 5b).

The coseismic rupture displacements rarely exceed 26 cm, remaining mostly lower than 16 cm (Figures 5a and 5b). Differently, the coseismic free face displacements are generally higher, in the range of 14–20 cm. Because the values of the measurements do not follow a normal distribution, but are rather characterized by different modal peaks (insets of Figures 5a and 5b), we use the median as the most representative value of each data set (details in Figure S1 in the supporting information). In general, both vertical dislocations and open cracks show the maxima located along the Cima del Redentore fault section and have median values of 10 cm and 8 cm, respectively (Figure 5c). The general offset distribution, neglecting some outliers, resembles a bell-shaped curve, apart from a local minimum just south of Mount Vettoretto. We found a weak positive

Figure 4. Coseismic ruptures (red arrows) along the VFS (Figure 2a for location). (a) Rupture affecting both soil and bedrock joint; (b) rupture cutting a small debris cone; (c) free face along the bedrock fault plane; (d) dislocation line affecting the slope debris; (e) coseismic rupture following a slice of fault breccia; (f) continuous and narrow rupture at the hanging wall of the bedrock fault plane.

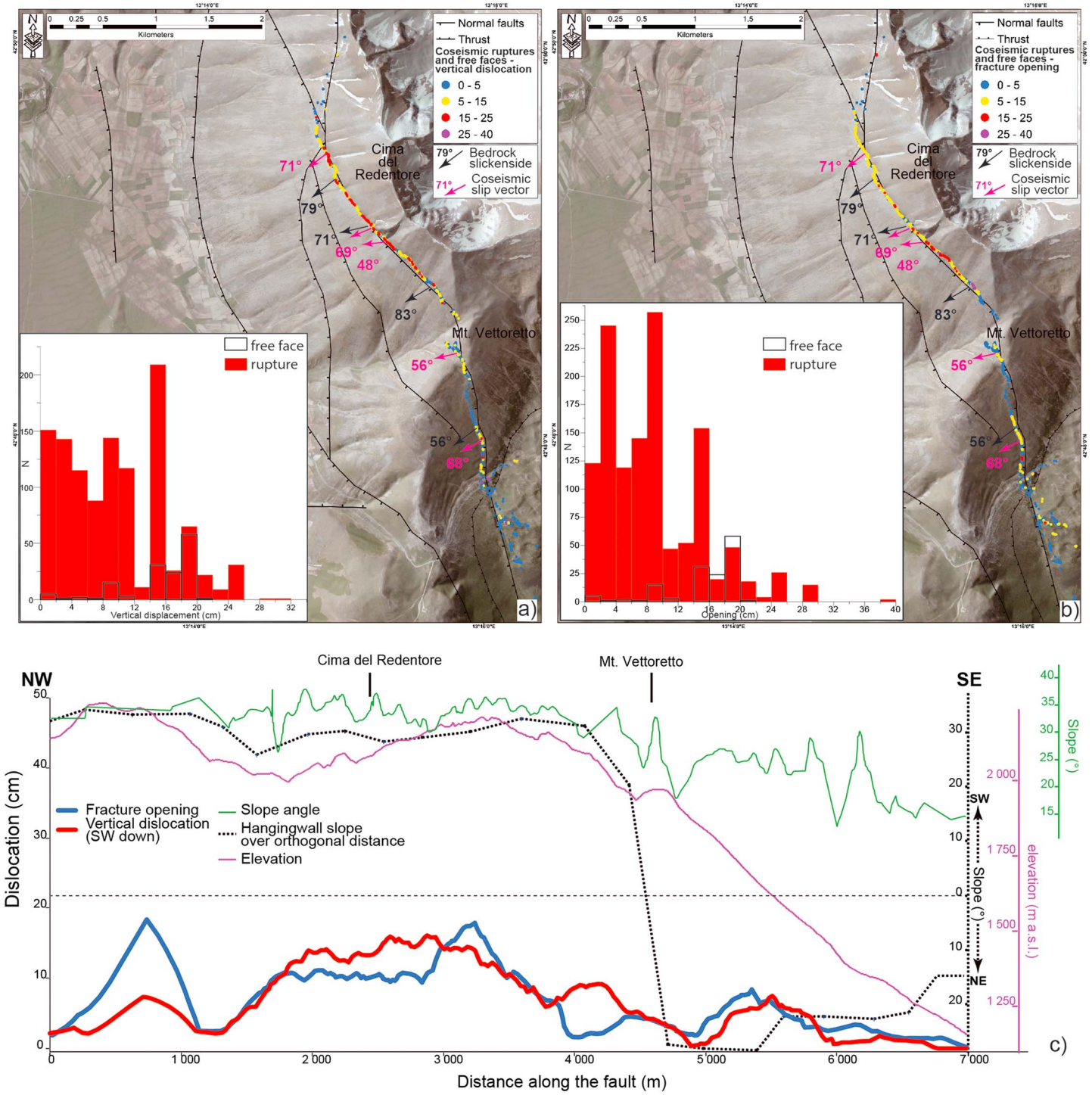

Figure 5. Spatial pattern of the coseismic displacements. Distribution and magnitude of (a) vertical dislocation and (b) opening values [*EMERGEO Working Group*, 2016, modified]. The slip and bedrock slickenside vectors with dip angle are reported. The insets show the frequency histograms of the vertical displacements and opening for ruptures affecting loose deposits (coseismic rupture) and along preexisting bedrock fault planes (coseismic free face); (c) along-strike distribution of the displacements (running average window of 400 m; details in Figure S1 in the supporting information). We report the absolute elevation of the coseismic ruptures (blue line) along with the angle of both maximum local slope (green line) and slope over the orthogonal distance from the fault, at the hanging wall (black line).

correlation between the components of displacement and both absolute elevation and average local slope angle (Figure S2). Notably, south of Mount Vettoretto, the slope over the orthogonal distance at the rupture hanging wall faces to the northeast (i.e., antislope). Here its opposite direction with respect to the coseismic slip rules out possible local gravitational contributions (Figure 5c).

4. Discussion and Conclusions

Soon after the 24 August 2016 Amatrice earthquake, the *EMERGEO Working Group* [2016] carried out a geological survey to collect data on the characteristics and distribution of the coseismic effects over the earthquake sequence area in order to ascertain the presence of primary surface faulting. As a result, we identified two sectors with contrasting features: the Laga Mountains Fault System (LFS) to the south, with few discontinuous coseismic ruptures, confined along its northern section, characterized by small offsets and prevalent fractures with irregular geometric patterns; the Mount Vettore Fault System (VFS) sector to the north, with a ~5.2 km long alignment of abundant ruptures, organized in a regular structural pattern.

In particular, along the eastern fault splay of the VFS, the ruptures alignment runs with an average N155° strike and constant kinematics (SW side down; Figure 5) at the base of a preexisting, SW dipping active normal fault, which exhibits a long-term geomorphologic and geologic expressions (i.e., ~ 20 m high Quaternary fault scarp and >500 m of net offset, respectively; Figure 2b). Also, the kinematics of the coseismic ruptures is comparable with that of the hosting normal fault (Figures 5a and 5b). Here the set of coseismic ruptures is localized and shows a general regularity of the structural pattern, which discloses a right stepping en échelon arrangement (Figure 3). The averaged along-strike distribution of the dislocation is quite regular, showing maxima of both vertical and horizontal components in coincidence with the southwestern flank of Cima del Redentore. Here the overall movement is quasi coaxial with the direction of maximum slope that presents values close to the critical angle of repose of granular deposits (~35°) (Figure 5c). However, the anticorrelation between the dislocation and the slope values suggests that only part of the observed displacement is due to slumps that occurred on the shallow continental deposits (Figures 5c and S1).

Summarizing, structural pattern, kinematics, and offset distribution appear to be independent from topography (elevation change, Figure 5c), morphology (e.g., erosional scarps and debris cone crosscut, Figure 3), and change in slope (Figure 5c). Also, the rupture characteristics disregard both bedrock and different bodies of unconsolidated deposits.

Along the VFS sector, all the features suggest that most of the observed displacement is due to primary surface faulting (i.e., propagation to the surface of the seismogenic fault plane motion at depth). Shallow gravitational effects may have locally contributed to a part of the observed deformation (for a maximum of ~10 cm, given the deviation from the average distribution of the displacements; Figure S1), while no evident features affecting the fault hanging wall point to a deep-seated gravity-driven deformation (e.g., lateral spreading, tilting, transverse and radial cracks, minor accessory scarps, curvilinear crown, and toe swelling).

Conversely, along the northern portion of the LFS, the coseismic rupture at depth did not propagate to the surface, possibly because of quasi-plastic mechanical properties of the outcropping thick Miocene flysch (1.0–2.0 km of calcareous marls, marly clay, and arenaceous pelites).

Notably, the surface projection of the SW dipping nodal plane of the focal mechanism of the M_w 6.0 main shock points to the coseismic rupture observed at the surface along the eastern fault splay of the VFS, suggesting a depth-surface connection (Figure 2). In this view, also the western splays of the VFS, although they present sparse secondary coseismic ruptures at the surface, may reveal a reactivated hanging wall volume, contributing to a complex far-field dislocation. Interestingly, to the south, the primary coseismic rupture ends at the intersection with the Mount Vettore thrust, suggesting that it could have played a role in stopping the rupture propagation (Figure 1).

Finally, a further element supporting the VFS primary surface faulting comes from the comparison with the updated scaling law relationships [*Wells*, 2015] (Figure 6). Both surface rupture length (~5.2 km) and average surface displacement (~13 cm of net dip slip by considering the median values of the vertical and the horizontal components) fit well the predicted estimates and are consistent with other worldwide surface rupturing earthquakes. Within the limits of the aleatory variability of input data, the average surface displacement is slightly higher than the predicted value possibly due to the contribution of shallow gravitational movements.

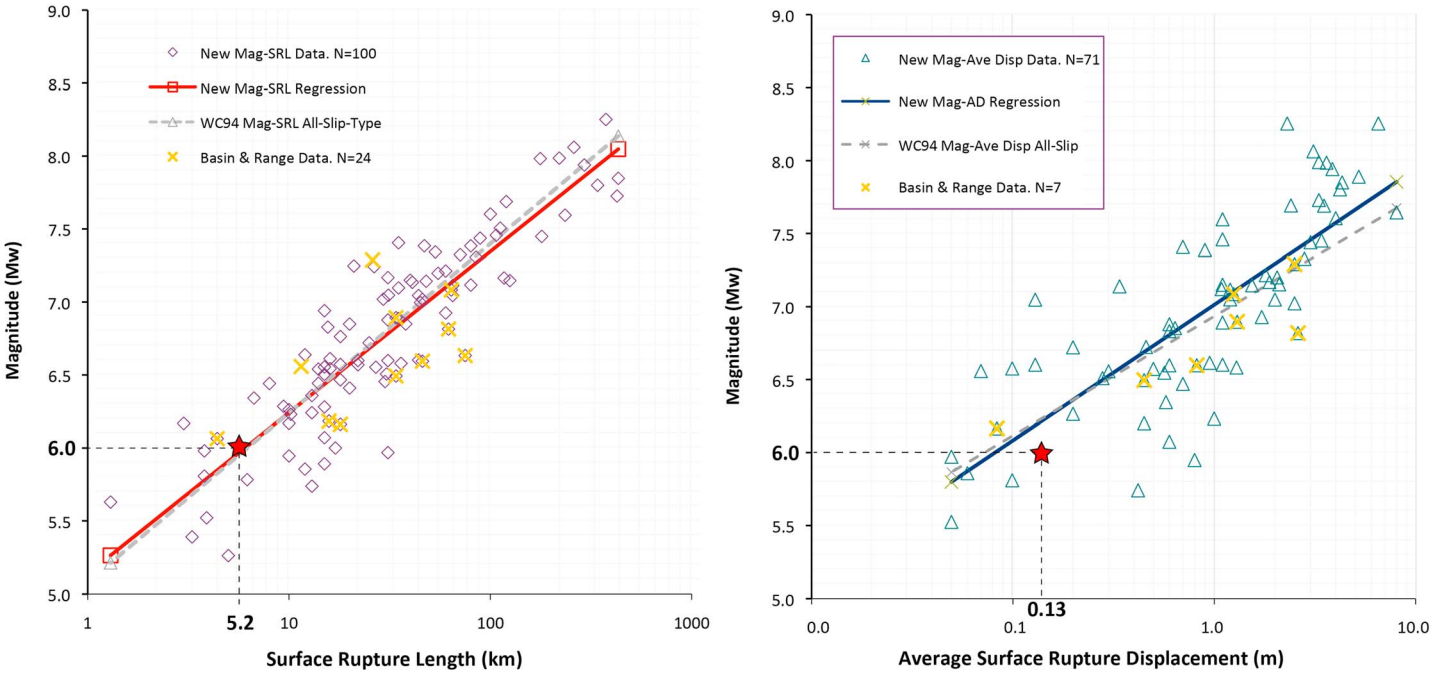

Figure 6. Updated empirical all-slip-type relationships between magnitude and surface rupture length/average surface displacement [*Wells*, 2015]. Red stars indicate the 2016 coseismic surface rupture.

As a whole, this study suggests that ~6.0 M_w normal-faulting earthquakes in the Apennines can be capable of rupturing the surface. Our interpretation, based on the data set referring to the sole earlier 24 August seismic event, may be verified by the surface coseismic effects framework induced by the subsequent October's earthquakes.

In this view, the 2016 Amatrice earthquake provides new data and insights for surface faulting in extensional domains, contributing to implement the worldwide database of the moderate earthquakes (SURFACE—SURface FAulting Catalogue Earthquakes, INQUA project 2016–2019).

A detailed comparison with other geophysical data like seismicity relocations, strong motion waveform modeling, and ground deformation satellite data (InSAR and GPS) will help in better understanding and evaluating the gravitational contribution versus the tectonic displacement.

Acknowledgments
This work was funded in the framework of DPC-INGV 2012–2021 (All. A) agreement. All data and software are freely available upon request to the authors. Thanks to Elisa Tinti for the precious help with the data analysis.

References

AMA_LOC Working Group (2016), Amatrice 2016 main events re-location (v1.0-20160902 12.00), Istituto Nazionale di Geofisica e Vulcanologia, doi:10.5281/zenodo.61371.

Atzori, S., I. Hunstad, M. Chini, S. Salvi, C. Tolomei, C. Bignami, S. Stramondo, E. Trasatti, A. Antonioli, and E. Boschi (2009), Finite fault inversion of DInSAR coseismic displacement of the 2009 L'Aquila earthquake (central Italy), *Geophys. Res. Lett.*, *36*, L15305, doi:10.1029/2009GL039293.

Azzaro, R., et al. (2016), The 24 August Amatrice 2016 earthquake: Macroseismic survey in the damage area and EMS intensity assessment, *Ann. Geophys.*, *59*, 8, doi:10.4401/ag-7203.

Cello, G., G. Deiana, L. Ferelli, L. Marchegiani, L. Maschio, S. Mazzoli, A. Michetti, L. Serva, E. Tondi, and T. Vittori (2000), Geological constraints for earthquake faulting studies in the Colfiorito area (central Italy), *J. Seismol.*, *4*, 357–364.

Centamore, E., et al. (1992), Carta geologica dei bacini della Laga e del Cellino e dei rilievi carbonatici circostanti, in *Studi Geologici Camerti*, Vol. Spec., Università degli Studi, Dipartimento di Scienze della Terra, SELCA, Firenze.

Cinti, F. R., L. Cucci, F. Marra, and P. Montone (1999), The 1997 Umbria-Marche (Italy) earthquake sequence: Relationship between ground deformation and seismogenic structure, *Geophys. Res. Lett.*, *26*, 895–898, doi:10.1029/1999GL900142.

D'Agostino, N. (2014), Complete seismic release of tectonic strain and earthquake recurrence in the Apennines (Italy), *Geophys. Res. Lett.*, *41*, 1155–1162, doi:10.1002/2014GL059230.

DePolo, C. M., D. G. Clark, D. B. Slemmons, and A. R. Ramelli (1991), Historical surface faulting in the Basin and Range province, western North America: Implications for fault segmentation, *J. Struct. Geol.*, *13*(2), 123–136.

EMERGEO Working Group (2010), Evidence for surface rupture associated with the M_w 6.3 L'Aquila earthquake sequence of April 2009 (central Italy), *Terra Nova*, *22*(1), 43–51, doi:10.1111/j.1365-3121.2009.00915.x.

EMERGEO Working Group (2012), Technologies and new approaches used by the INGV EMERGEO Working Group for real time data sourcing and processing during the Emilia Romagna (northern Italy) 2012 earthquake sequence, *Ann. Geophys.*, *55*(4), 2012, doi:10.4401/ag-6117.

EMERGEO Working Group (2016), Coseismic effects of the 2016 Amatrice seismic sequence: First geological results, *Ann. Geophys.*, *59*(5), doi:10.4401/ag-7195.

Galadini, F., and P. Galli (1999), The Holocene paleoearthquakes on the 1915 Avezzano earthquake faults (central Italy): Implications for active tectonics in the central Apennines, *Tectonophysics*, *308*(1), 143–170.

Galli, P., F. Galadini, and D. Pantosti (2008), Twenty years of paleoseismology in Italy, *Earth Sci. Rev.*, *88*, 89–117.

Pantosti, D., and G. Valensise (1990), Faulting mechanism and complexity of the November 23, 1980, Campania-Lucania earthquake, inferred from surface observations, *J. Geophys. Res.*, *95*(B10), 15,319–15,341, doi:10.1029/JB095iB10p15319.

Pierantoni, P., G. Deiana, and S. Galdenzi (2013), Stratigraphic and structural features of the Sibillini Mountains (Umbria-Marche Apennines, Italy), *Ital. J. Geosci.*, *132*(3), 497–520.

Pizzi, A., F. Calamita, M. Coltorti, and P. Pieruccini (2002), Quaternary normal faults, intramontane basins and seismicity in the Umbria-Marche-Abruzzi Apennine Ridge (Italy): Contribution of neotectonic analysis to seismic hazard assessment, *Boll. Soc. Geol. Ital.*, *1*, 923–929.

Rovida, A., M. Locati, R. Camassi, B. Lolli, and P. Gasperini (Eds.) (2016), *CPTI15, The 2015 Version of the Parametric Catalogue of Italian Earthquakes*. Istituto Nazionale di Geofisica e Vulcanologia, Rome, Italy, doi:10.6092/INGV.IT-CPTI15.

Stirling, M., T. Goded, K. Berryman, and N. Litchfield (2013), Selection of earthquake scaling relationships for seismic-hazard analysis, *Bull. Seismol. Soc. Am.*, *103*(6), 2993–3011, doi:10.1785/0120130052.

Vai, G. B., and L. P. Martini (Eds.) (2001), *Anatomy of an Orogen: The Apennines and Adjacent Mediterranean Basins*, pp. 633, Kluwer Acad., Dordrecht, Netherlands.

Valoroso, L., L. Chiaraluce, D. Piccinini, R. Di Stefano, D. Schaff, and F. Waldhauser (2013), Radiography of a normal fault system by 64,000 high-precision earthquake locations: The 2009 L'Aquila (central Italy) case study, *J. Geophys. Res. Solid Earth*, *118*, 1156–1176, doi:10.1002/jgrb.50130.

Wells, D. (2015), Issues and approaches for estimating M_{max} for earthquake sources in the Basin and Range Province, in *Proceedings Volume, Basin and Range Province Seismic Hazards Summit III: Utah Geological Survey Miscellaneous Publication 15–5*, edited by W. R. Lund, variously paginated, DVD, Salt Lake City, Utah.

Wells, D. L., and K. J. Coppersmith (1994), New empirical relationships among magnitude, rupture length, rupture width, rupture area, and surface displacement, *Bull. Seismol. Soc. Am.*, *84*(4), 974–1002.